17th World Conference on Earthquake Engineering, 17WCEE
Sendai, Japan - September 13th to 18th 2020

EFFECTS OF MULTI-DIRECTIONAL SEISMIC INPUT ON THE DYNAMIC BEHAVIOR OF URM STRUCTURES: AN EXPERIMENTAL STUDY

S. Kallioras [1], F. Graziotti [2], L. Grottoli [3], A. Penna [4], G. Magenes [5]

[1] *Postdoctoral Researcher, University of Pavia, Department of Civil Engineering and Architecture (DICAr) & European Centre for Training and Research in Earthquake Engineering (EUCENTRE), Pavia, Italy, stylianos.kallioras@unipv.it*
[2] *Assistant Professor, University of Pavia, DICAr & EUCENTRE, Pavia, Italy, francesco.graziotti@unipv.it*
[3] *Researcher, EUCENTRE, Pavia, Italy, luca.grottoli@eucentre.it*
[4] *Associate Professor, University of Pavia, DICAr & EUCENTRE, Pavia, Italy, andrea.penna@unipv.it*
[5] *Professor, University of Pavia, DICAr & EUCENTRE, Pavia, Italy, guido.magenes@unipv.it*

Abstract

This paper presents an experimental study aimed at evaluating the influence of the vertical acceleration component of ground motions on the dynamic response of unreinforced masonry buildings. The research was motivated by recent post-earthquake observations of greater structural damage at sites near the fault, where horizontal and vertical ground motions were strong and well synchronized. Vertical accelerations can result in the fluctuation of gravity loads, which, in turn, control the in-plane lateral load capacity of masonry walls due to variation of friction forces between units and mortar. Also, the simultaneous application of horizontal and vertical accelerations could affect the out-of-plane rocking stability of slender walls. Such phenomena seem not to be sufficiently explained in the existing literature, while experimental evidence is undoubtedly missing. In this study, the damage potential of the vertical accelerations to masonry buildings was investigated through a series of multi-directional shake-table tests on masonry structures under simulated near-fault ground motions of increasing intensity. The experiments included a set of three identical building specimens, subjected to the principal horizontal component only, the horizontal component combined with the vertical one, and to the full three-component ground motion, respectively. The test structures comprised gable walls, chimneys, and parapets, which appear to be more sensitive to variations in gravity loads. These experiments are expected to provide significant experimental evidence for the consideration of the vertical ground motion in the seismic assessment and design of masonry buildings. All data from the tests are available upon request on www.eucentre.it/nam-project.

Keywords: shake-table tests; unreinforced masonry; vertical acceleration; out-of-plane rocking; non-structural damage

1. Introduction

The experiments presented in this paper were part of an extensive experimental campaign that started in 2014 with the aim to assess the seismic vulnerability of unreinforced masonry buildings (URM) in the Groningen region of the Netherlands [1]. The area, historically not prone to tectonic ground motions, during the last two decades, has been hit by small-magnitude earthquakes induced by the local natural gas production activities and consequent reservoir depletion [2].

The research discussed below was motivated by the need to investigate the effects of the combined horizontal and vertical acceleration components of ground motion on the dynamic response of URM structures and non-structural masonry elements, such as chimneys, gables, and parapets. Vertical accelerations result in the fluctuation of wall axial loads, which, in turn, control the flexural and shear capacity of masonry piers. Downward accelerations entail instantaneous decrement of frictional resistance of masonry walls, which can lead to a potential increment of sliding between the bricks in case of simultaneous horizontal seismic action of considerable intensity [3][4].

Some of the past shake-table tests on full-scale URM buildings highlighted the considerable influence of the boundary conditions of walls on their in-plane and out-of-plane response [5][6][7][8]. The tests showed that wall boundary conditions might vary during an earthquake due to damage cumulation, interaction with floors and orthogonal walls, but also due to the presence of vertical accelerations. The simultaneous application of horizontal and vertical accelerations could affect the out-of-plane rocking stability of slender walls. Such phenomena seem not to be sufficiently explained in the existing literature, while only limited experimental research is currently available about the effect of multi-directional ground motions on the dynamic response of URM structures [6][7].

In this study, a series of multi-directional shake-table experiments were performed on three nominally identical URM buildings, considering different seismic input combinations, every time introducing one additional ground motion component. Specifically, the first specimen, labeled EUC-BUILD-8.1, was subjected to uni-directional shaking using a single horizontal acceleration component. The second specimen, labeled EUC-BUILD-8.2, was subjected to one horizontal acceleration component combined with the vertical one, while the last one, termed EUC-BUILD-8.3, was tested under a full three-component motion. Two different ground-motion records were employed to evaluate the effects of both tectonic and induced seismicity scenarios.

The building specimens simulated a single-story clay-brick structure with asymmetric façades and a flexible timber diaphragm. The prototype included various structural and non-structural elements that might exhibit sensitivity to variations in gravity loads under seismic excitation, such as piers of various aspect ratios subjected to in-plane loads, slender walls under one-way out-of-plane bending action, as well as parapets, gables, and chimneys, which are vulnerable to out-of-plane overturning. Plaster coating was applied to the interior of the buildings to assess aesthetic damage to the walls.

This paper summarizes the main characteristics of the specimens and the major observations from the shake-table experiments, illustrating the activated damage mechanisms and the overall performance of the buildings.

2. Specimens overview

The three test buildings were identical in geometry and construction details. They were characterized by a 2.82-m floor height, with a 1.95-m-high gable wall, two chimneys of different heights, and three parapets extending over the floor level (Fig. 1a). The overall footprint dimensions were 4.25 m in the longitudinal building direction (i.e., North-South), 4.04 m in the transverse one (i.e., East-West), and the walls were built in a rectangular layout (Fig. 1b and c).

The load-bearing structural system consisted of unreinforced masonry walls. They were constructed employing 208×100×50 mm^3 solid clay bricks shipped from the Netherlands, and 10-mm-thick, fully mortared head- and bed-joints, using mortar produced in Italy. The same batches of materials were used for all three structures in a way to reduce the variability in the mechanical characteristics among the specimens.

Three out of the four perimeter walls, North, East, and West façades, consisted of a single 100-mm-wide leaf, built with the standard stretcher bond. The South facade was made of a double 208-mm-thick wythe, using the Dutch cross brickwork bond. Large asymmetric openings were present at all façades, resulting in varying wall areas in both building directions, with the intent to magnify differential wall displacements (Fig. 1d). Timber lintels were placed above all openings: they were 110-mm-deep timber beams, extending into the masonry 100 mm on each side of the openings for support (Fig. 2a).

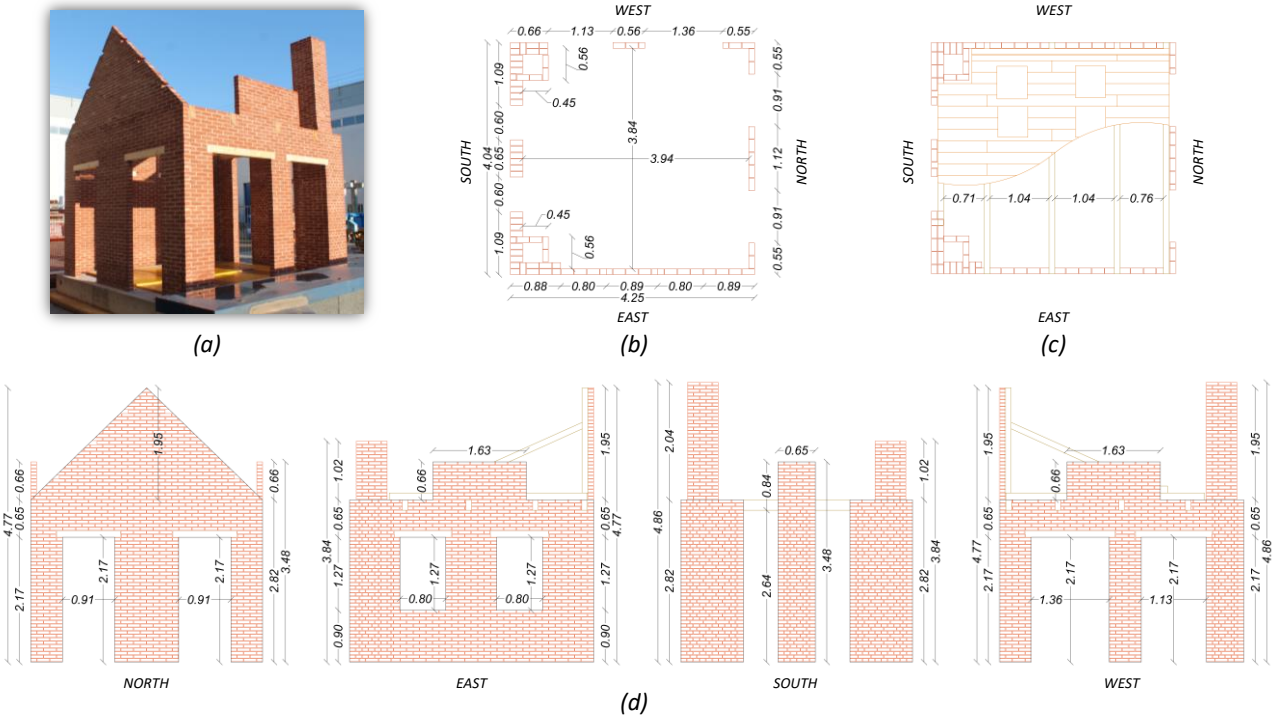

Fig. 1 – Full-scale building specimens: (a) North-West view; (b) ground-floor plan; (c) floor framing plan; (d) elevation views (units of m).

The floor consisted of 30-mm-thick timber floorboards nailed to 100-mm-wide and 180-mm-deep timber joists by means of two nails at each intersection, resulting in a flexible diaphragm (Fig. 2b). The floor joists were supported by the East, West, and South walls, while there were no wall-to-diaphragm connections at the North building façade. At the end of the construction works, 8-mm-diameter steel anchors were installed at the gable-floor joints, as shown in Fig. 2c (also visible in Fig. 2e). These anchors were not connected to the timber floor initially, but they were placed with the possibility to be nailed subsequently, in case of the early development of an out-of-plane mechanism of the façade.

A timber truss was installed back to back with the gable wall in a way that allowed only a one-side rocking response of the latter. Struts were additionally provided to support the truss rafters and transfer to the floor frame loads coming from the impact of the gable wall on the truss (Fig. 2d). A timber plate was installed outside the gable, forming an end-plate that prevented the collapse of the gable due to out-of-plane overturning during the experiments. Initially, the plate was placed at a distance that allowed relative displacements between gable and roof truss up to 170 mm; it was suspended by the roof truss through 20-mm-diameter steel bars (Fig. 2e).

The building specimens included two vertical URM chimneys on the South façade: one was interlocked with the West wall, while the second one was built together with the East wall. The two chimneys were designed to have the same flue, 340×340 mm^2. The chimney on the West side was moderately slender, extending approximately 2.0 m above the floor, while the East chimney was squatter as it penetrated the floor for 1.0 m (Fig. 2f). Three 0.66-m-tall parapets were built on top of the East, West, and South walls, as illustrated in Fig. 1d, and Fig. 2f.

The interior face of the walls at the first story was coated with conventional plaster to facilitate detecting the cracks during the post-test damage surveys, and to assess the effects of shaking on both structural and non-structural damage of the walls (Fig. 2g).

Eight 500×500 mm^2 openings were foreseen on the floor sheathing to avoid interference with the columns of a steel-framed structure installed in the interior of the buildings (visible in Fig. 2i). The steel structure served as a reference frame for the measurement of relative displacements and as a safety system protecting the shake table against impact due to structural collapse during the tests. Each specimen was constructed on a reinforced concrete foundation beam, which was tightly bolted to the shake table. The foundation weighed 10.6 t, and it was rigid enough to allow the transportation of the structures from the construction site onto the shake table without causing damage to the masonry walls (Fig. 2h).

Fig. 2 – Construction details of the building specimens: (a) timber lintels at West façade; (b) floor diaphragm during construction; (c) wall-to-diaphragm connections at North façade (initially deactivated); (d) truss and struts at North gable; (e) end-plate outside the North gable (initially at distance); (f) chimneys and parapets (South-East view); (g) rendering of building interior; (h) transportation of building specimens; (i) additional masses on the floor diaphragm (top East view).

The masonry walls had a mass of 11.3 t, estimated with a mean density of 1950 kg/m^3. Floor diaphragm and roof truss provided a mass of 0.3 t. An additional mass of 1.1 t was placed on the floor, using 44 25-kg-heavy bags of mortar (Fig. 2i), evenly distributed over the diaphragm to account for superimposed dead and live loads (equivalent to approximately 67 kg/m^2). Two extra loads, equal to 450 kg each, were placed at the East and West borders of the floor to simulate the self-weight of the missing roof, which would have been transferred to the longitudinal walls of the structure through trusses supported on the East and West edges of the floor diaphragm. The total mass of the prototype building was 13.6 t.

The three buildings suffered slight damage during the construction period: minor cracking was detected at the supports of the floor joists and the lintels, due to the contraction of both the timber and the early-age mortar, and the weak cohesion developed between them.

3. Instrumentation plan

The instrumentation consisted of 65 accelerometers (Fig. 3a), 22 linear, and 17 wire potentiometers (Fig. 3b), mounted on each specimen to monitor its dynamic response during the tests in both horizontal and vertical directions. The steel frame inside the building served as a rigid reference system for the measurement of displacements of the floor, the walls, and the non-structural masonry elements above the floor (i.e., gable wall, parapets, chimneys) with respect to the shake table. Additional accelerometers and displacement transducers were installed on the shake table to record the applied table accelerations and displacements. A three-dimensional optical motion-capture system allowed to obtain descriptions of local deformations and global displacements of each building during the earthquake simulations [9]: cameras recorded the in-plane and out-of-plane displacements of the South, West, and North building façades by monitoring the motion of passive spherical markers coated with a retro-reflective material, which were placed on the walls (Fig. 3c).

The earthquake-simulation tests were covered by high-definition video cameras mounted around but also inside the specimen. All data and video recordings from the experiments are available upon request on www.eucentre.it/nam-project. For a thorough description of the measurements acquired in the lab, the reader is referred to the research report [10].

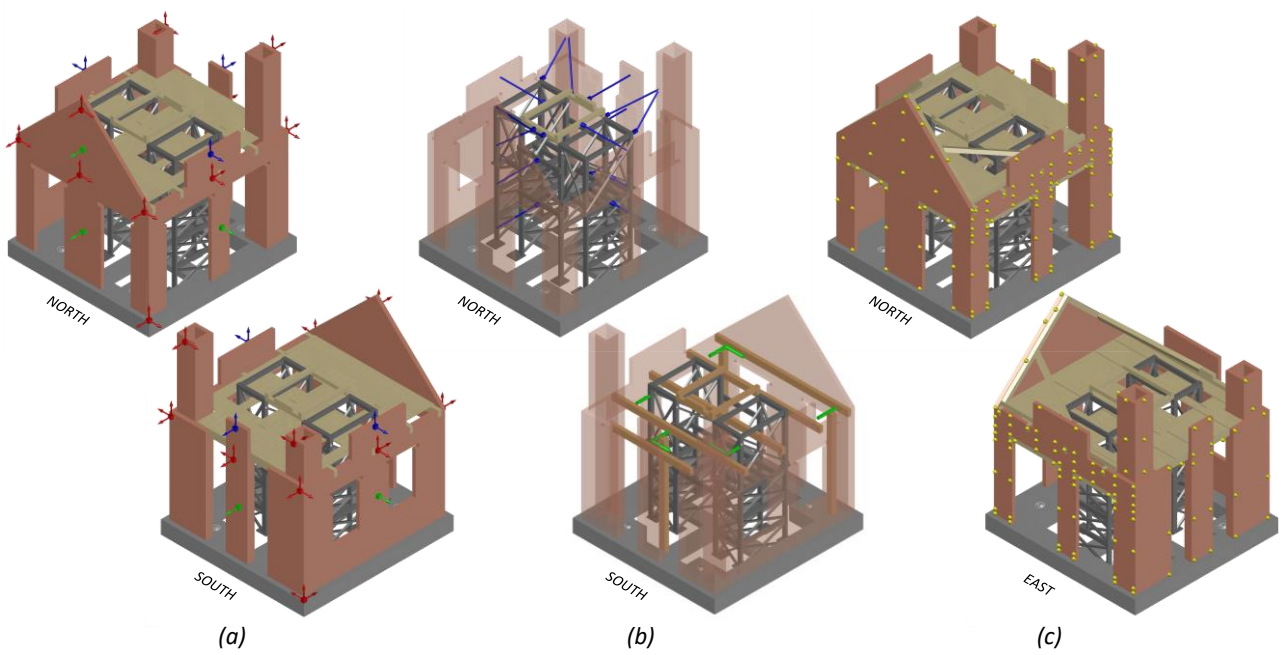

Fig. 3 – Instrumentation plan: (a) 3D, 2D, and 1D accelerometers; (b) linear and wire potentiometers; (c) points monitored by the 3D optical motion-capture system.

4. Seismic input motions

The test buildings were subjected to cumulative incremental dynamic tests, applying a series of shake-table motions of increasing intensity to assess damage evolution, failure modes, and ultimate capacity of the structures. The same seismic input motions were employed for all shake-table experiments, every time introducing one additional motion component. Specifically, EUC-BUILD-8.1 was subjected to single-component motions (i.e., only horizontal input acceleration; Fig. 4a), EUC-BUILD-8.2 was subjected to two-component motions (i.e., combined horizontal and vertical input accelerations; Fig. 4b), while EUC-BUILD-8.3 was tested under the full three-component ground motions (Fig. 4c). This allowed the direct comparison among the test results and the evaluation of the effects of the multi-directional seismic input on the response of the buildings.

Two different real earthquake scenarios were considered in the experiments: ground motions due to anthropogenic and tectonic activity. The first scenario, termed SC1, was a three-component, pulse-like acceleration recording from the 2018 Zeerijp Earthquake in the Groningen gas field of the Netherlands [11][12]. Production-induced earthquakes are typically characterized by shallow depth and low magnitude; consequently, they generate ground motions that usually have comparable vertical-to-horizontal motion intensities but a low amplitude and short duration. Also, the short source-to-site distance results in a considerable time interval between vertical and horizontal motions, with the vertical accelerations always preceding. As such, the vertical and horizontal ground-motion components of record SC1 were not well synchronized or strong enough to cause significant structural damage. The second ground-motion scenario, termed SC2, was a three-component motion recorded near the causative fault of the October 26 event nearby Macerata during the 2016 Central Italy earthquake sequence. This ground motion was carefully selected [13], so that vertical and horizontal acceleration components have high amplitude and coincident peaks to test the influence of vertical accelerations on the structural response.

Table 1 lists the characteristics of the two selected ground motions. Fig. 5 illustrates the theoretical acceleration time-series of the input motions and their elastic pseudo-acceleration response spectra at 5% viscous damping ratio. All dynamic tests were performed by applying the principal horizontal acceleration component (i.e., *X* component) in the direction perpendicular to the gable wall.

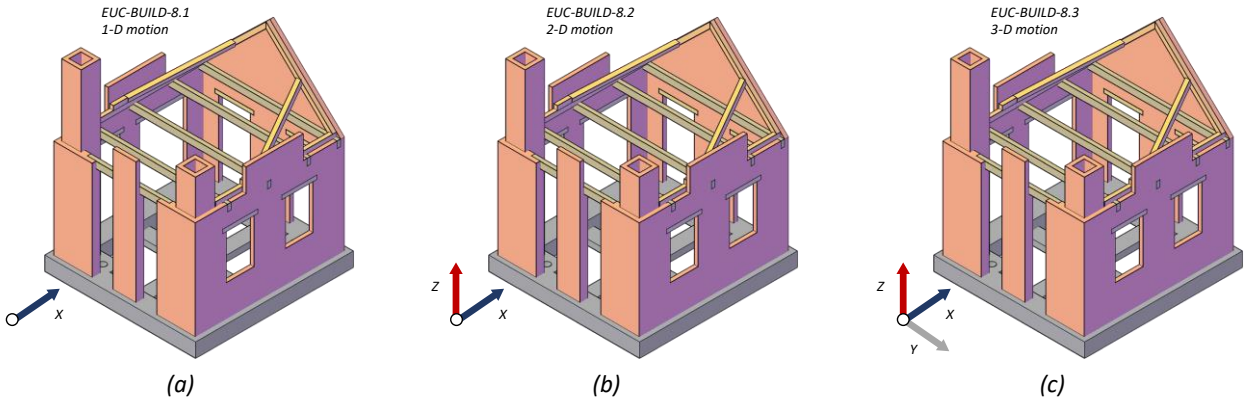

Fig. 4 – Incremental dynamic tests applying: (a) uni-; (b) bi-; (c) tri-directional seismic excitations.

The input signals were scaled in amplitude to obtain the desired incremental test protocol, consisting of nine earthquake simulations. Record SC1 was scaled in acceleration amplitude at 50%, 100%, and 150%; SC2 was nominally scaled at 25%, 50%, 75%, 100%, 150%, and 200%. As each signal was linearly scaled, its significant duration remained unchanged: signals SC1-100% and SC2-100% had 5-75% significant durations, $D_{s,5\text{-}75}$, equal to 0.43 s and 1.87 s, respectively. In-between those tests, the specimens were subjected to low-amplitude random excitations, covering a broad frequency range (0.1-40 Hz) with consistent energy content for the dynamic identification of the structures.

Table 1– Summary of the selected input ground motions.

Event	Date & time	Station	M_W	R_{ep} [km]	D [km]	PGA_V/PGA_H* [-]	$\Delta t_{IA,5\%}$† [s]
Zeerijp (NL)	08/01/2018, 14:00:52	Garsthuizen (BGAR)	3.4	2.5	3.0	0.64	1.97
Macerata (IT)	26/10/2016, 19:18:06	Montecavallo (MCV)	5.9	14.0	7.5	0.88	0.22

* PGA_V/PGA_H: ratio of peak vertical to peak horizontal ground acceleration; indicator for the magnitude of the relative instantaneous intensity of the vertical ground motion with respect to horizontal ground motion.

† $\Delta t_{IA,5\%}$: time difference between the 5% accumulation of Arias intensity of vertical and horizontal ground motions; indicator for the synchronization between the vertical and horizontal ground motions.

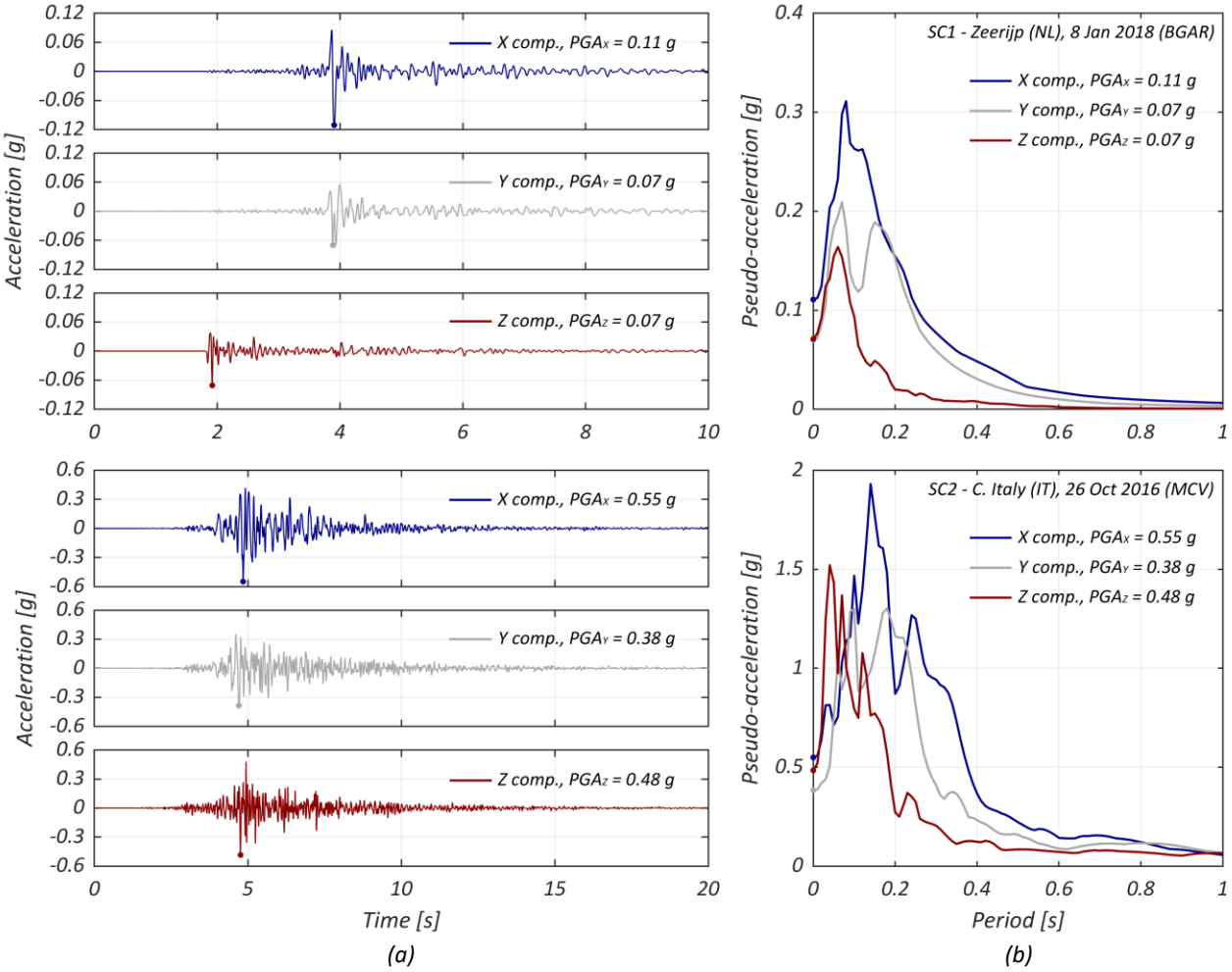

Fig. 5 – Input motions SC1 and SC2: (a) acceleration time-series; (b) elastic pseudo-acceleration response spectra for 5% viscous damping ratio.

5. Test results

EUC-BUILD-8.1 and EUC-BUILD-8.3 did not suffer any significant structural damage for testing under earthquakes SC1 (i.e., up to test SC1-150%, with nominal PGA_X = 0.17 g). The first noteworthy damage appeared in EUC-BUILD-8.2 during test SC1-100% (PGA_X = 0.11 g); for specimens EUC-BUILD-8.1 and EUC-BUILD-8.3, the first significant damage was observed only after tests SC2-25% (PGA_X = 0.14 g) and SC2-50% (PGA_X = 0.27 g), respectively.

The North gable wall of all buildings exhibited high vulnerability in out-of-plane overturning, reaching deflections at the top of approximately 10 cm by the end of test SC2-75% (PGA_X = 0.41 g). Shaking at higher intensities would have caused the collapse of the gable, leading to the premature termination of the experiments. Therefore, before proceeding with tests SC2-100% (PGA_X = 0.55 g), the North façade was retrofitted by activating the wall-to-diaphragm connectors provided at the floor level, and the timber plate installed outside the gable, as detailed in Section 2. All three specimens were considered at near-collapse state after testing under input motion SC2-200% (nominal PGA_X = 1.1 g).

After every earthquake simulation, structural and non-structural damage were thoroughly assessed, and cracks were accurately mapped. Fig. 6 illustrates the overall crack pattern as seen from the external face of the building walls after completion of the test sequence (i.e., after test SC2-200%).

The following sections illustrate the seismic performance of the specimens, reporting qualitative damage observations and the developed damage mechanisms.

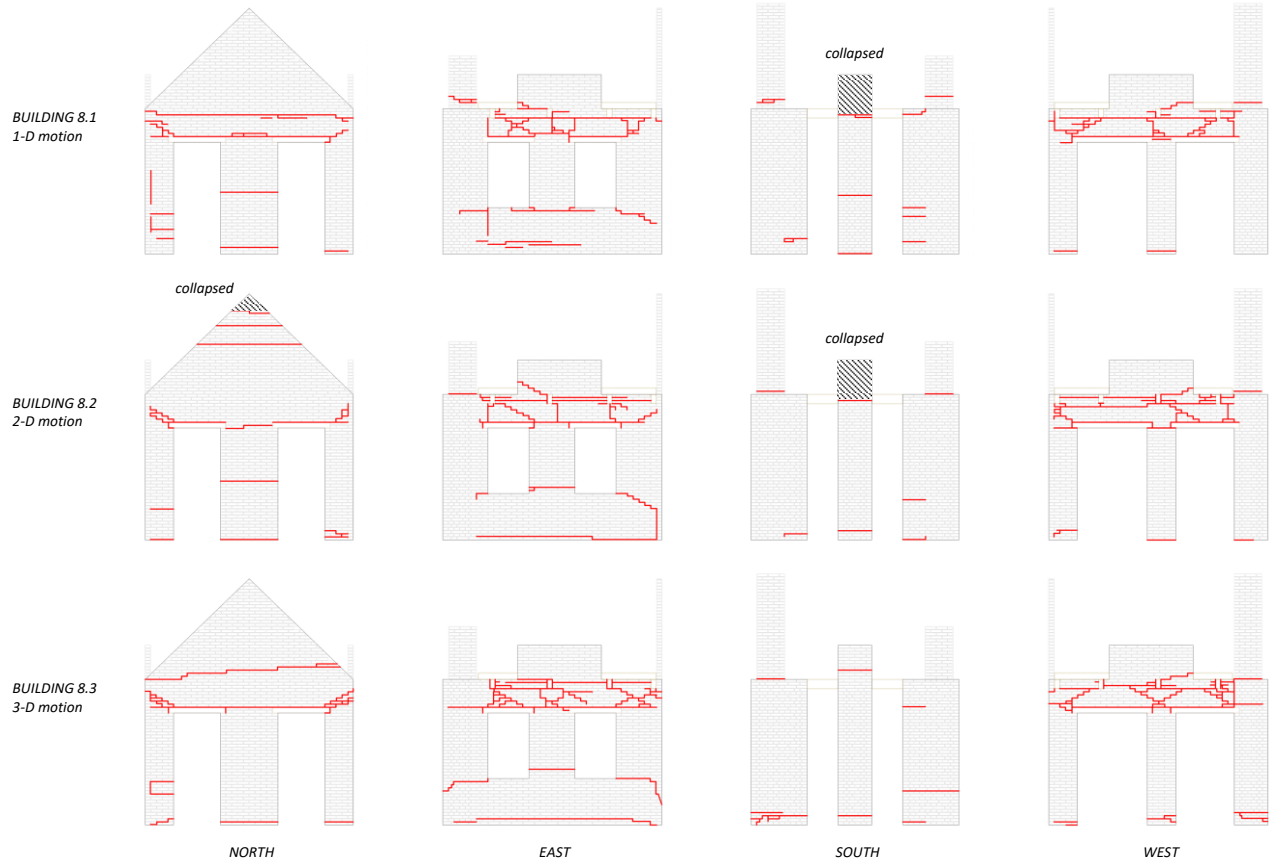

Fig. 6 – Observed crack pattern at the end of the test sequence (i.e., after test SC2-200%, with PGA_X = 1.1 g).

5.1 Observed damage after the SC1 motions

During testing under the SC1 input motions, scaled from 50% to 150% (nominal PGA_X from 0.06 g to 0.17 g), specimen EUC-BUILD-8.1 did not experience any visible damage, other than a few minor cracks above the timber lintels.

Shaking at SC1-100% (PGA_X = 0.11 g) caused considerable damage to EUC-BUILD-8.2 only; specifically: i) cracking of the North gable wall at the base (i.e., just above the openings) and the top; ii) flexural cracking at the base of the South parapet; iii) stair-stepped cracking on a spandrel at the West façade; iv) flexural cracking on the Northern pier of the West façade; v) hairline horizontal cracking at the bottom of the East façade due to the incipient activation of a shear-sliding mechanism. The latter mechanism also developed in EUC-BUILD-8.1 and EUC-BUILD-8.3 but in later steps of the experiments (i.e., at SC2-25% and SC1-150%, respectively).

The SC2 motions were sensibly stronger and put a significant strain on the structures.

5.2 Observed damage after the SC2 motions

5.2.1 EUC-BUILD-8.1

The first significant damage in EUC-BUILD-8.1 was identified after test SC2-25% (PGA_X = 0.14 g): horizontal flexural cracks developed at the bottom of all West piers, indicative of their in-plane rocking response. Failure also occurred at the slender South-West chimney: a horizontal crack cut through the entire stack a few centimeters above the floor diaphragm (Fig. 7a). At the North façade, a horizontal flexural crack developed at the bottom of the central pier due to out-of-plane bending action (Fig. 7b).

During shaking at SC2-50% (PGA_X = 0.27 g), new hairline diagonal cracks were seen at the spandrels of the West façade (Fig. 7c). At the same test, the formation of a horizontal crack at the base of the North gable wall indicated the activation of an out-of-plane overturning mechanism. Testing under SC2-75% (PGA_X = 0.41 g) caused the fracture at the base of the South parapet and the propagation of the pre-existing horizontal cracks at the North gable wall.

In the tests SC2-100% and SC2-150% (PGA_X = 0.55 g and 0.82 g, respectively), in-plane mechanisms developed at the piers of the East façade (Fig. 7d), which exhibited prevailing flexural-rocking behavior. Also, a horizontal flexural crack appeared at the bottom of the central pier of the South façade, while the South parapet collapsed.

The experiment was completed with the input motion SC2-200% (PGA_X = 1.1 g), which caused the brittle shear failure of the squat chimney at the level of the floor diaphragm (Fig. 7e), and the development of vertical one-way bending mechanisms at mid-height of both South and North central piers.

5.2.2 EUC-BUILD-8.2

In the case of EUC-BUILD-8.2, flexural cracks appeared at the bottom of the West piers for the first time during test SC2-25%. During test SC2-50%, a horizontal crack formed at mid-height of the gable wall, and the top third part tipped on the timber plate installed outside the gable (Fig. 7f).

After test SC2-75%, the pre-existing flexural cracks at the bottom of the west piers had propagated in the transverse building walls (i.e., South and North façades), and a horizontal flexural crack was formed at the bottom of the South central pier. During test SC2-100%, the observed damage did not change significantly.

Test SC2-150% caused the flexural cracking of the slender chimney at the floor-diaphragm level. This failure mode was developed only at this stage of the experiment (i.e., delayed in comparison to EUC-BUILD-8.1 and EUC-BUILD-8.3) due to the prior activation of a rocking response mechanism of the full height of the chimney, involving the entire South-West corner of the building. This failure caused residual crack widths of about 5 mm along the base of the chimney (Fig. 7g), and 30-mm-wide vertical cracks at the spandrels of the West façade (Fig. 7h).

Similar to EUC-BUILD-8.1, shaking at SC2-200% resulted in the development of in-plane flexural-rocking mechanisms at the piers of the East façade (Fig. 7i), and the shear failure of the squat chimney above the floor. An out-of-plane mechanism involved the upper portion of the North gable and resulted in rigid-body sliding: mortar joint sliding and block de-cohesion were observed along a major horizontal crack located around the level of the lintels, with a maximum residual of 80 mm (Fig. 7j).

5.2.3 EUC-BUILD-8.3

Specimen EUC-BUILD-8.3 exhibited first significant damage during shaking at SC2-50%: flexural cracks developed at the bottom of all West piers, and at the location where the slender chimney penetrated the floor diaphragm. Also, accelerations in the *Y* building direction caused the flexural cracking of the East parapet wall. Test SC2-75% did not induce damage to the structure, other than the flexural cracking of the South parapet above the floor.

Shaking at SC2-100% impaired considerable damage to EUC-BUILD-8.3, specifically: i) the formation of a horizontal cracking at the bottom of the South and North central piers due to the development of out-of-plane bending mechanisms (similar to EUC-BUILD-8.2); ii) diffuse cracking at the spandrels of East and West façades; iii) stair-stepped hairline cracking at the base of the North gable wall, despite having been subjected to prior retrofitting.

During test SC2-150%, horizontal hairline cracks developed at the top and bottom of the East piers, associated with their flexural-rocking behavior. Damage due to such in-plane rocking mechanism was cumulated at the West façade, as well: cracks at the top and bottom ends of the piers extended into the transverse building façades, reaching residual crack widths of 10-20 mm (Fig. 7k).

After the SC2-200% test, an out-of-plane mechanism was fully activated at the North building façade, similar to EUC-BUILD-8.2. Extensive damage was observed throughout the building, which was deemed to have reached near-collapse conditions.

Fig. 7 – Observed damage mechanisms: (a) flexural cracking of the slender chimney in EUC-BUILD-8.1; (b) flexural cracking due to out-of-plane bending at the North central pier of EUC-BUILD-8.1; (c) damage to the spandrels at the West façade of EUC-BUILD-8.1; (d) flexural cracks due to in-plane rocking mechanism at the East piers in EUC-BUILD-8.1; (e) shear failure of the squat chimney in EUC-BUILD-8.1; (f) collapse of the top part of the gable in EUC-BUILD-8.2; (g) flexural crack at the bottom of the slender chimney in EUC-BUILD-8.2; (h) vertical cracks due to detachment of the slender chimney at the West façade of EUC-BUILD-8.2; (i) damage due to in-plane rocking mechanism at the East piers of EUC-BUILD-8.2; (j) out-of-plane mechanism at the North building façade in EUC-BUILD-8.2; (k) damage due to rocking behavior of the West piers in EUC-BUILD-8.3.

6. Conclusions

This paper discussed the multi-directional shake-table experiments on three building specimens, simulating a full-scale unreinforced clay-brick masonry structure with a flexible diaphragm, a gable wall, chimneys, and parapets. A series of cumulative incremental dynamic tests were performed up to the near-collapse conditions of the specimens, using input ground motions representative of both induced and natural seismicity scenarios.

Real earthquake records were carefully selected to be strong enough and well synchronized to test the effects of multi-directional seismic input on the structural response. Different seismic input combinations were considered, introducing one additional ground-motion component as proceeding from experiment EUC-BUILD-8.1 (uni-directional horizontal excitation) to EUC-BUILD-8.2 (combined horizontal and vertical excitation), and eventually to EUC-BUILD-8.3 (tri-directional shaking).

The preliminary comparison of the test results showed that the vertical acceleration component did not seem to have a strong influence on the overall seismic performance of the building specimens. The failure modes and ultimate capacity of the three structures were similar. The displacement demands induced by the same shaking intensities were comparable; slight differences were observed in test EUC-BUILD-8.3, where the second horizontal motion component put some extra strain to the structure (probably due to the higher resultant horizontal acceleration), and caused torsional effects. All buildings reached near-collapse conditions for testing at 200% of the strong ground motion SC2, with nominal PGA_X = 1.1 g.

The three specimens exhibited similar damage mechanisms, specifically: i) flexural cracking of piers, and diffuse shear cracking of spandrels exclusively associated with the in-plane response of the East and West façades; ii) large deformability of the floor diaphragm due to significant differential displacements between parallel walls; iii) development of an out-of-plane overturning mechanism and consequent one-side rocking of the North gable wall (retrofit of the gable was required at the same shaking intensity – SC2-75% with nominal PGA_X = 0.41 g); iv) flexural failure above the floor diaphragm, and subsequent rocking response of the slender chimney and the parapet at the South façade. The overturning mechanism of the slender chimney occurred with a delay in EUC-BUILD-8.2 compared to the other two tests, but for reasons that do not seem to be associated with the seismic input (it was most probably due to local imperfections).

Nonetheless, in tests where vertical accelerations were applied (i.e., EUC-BUILD-8.2 and EUC-BUILD-8.3), signs of early damage were observed in slightly lower horizontal shaking intensities, when compared to the uni-directional tests (i.e., EUC-BUILD-8.1). Another difference in the response of the three buildings, which might be attributed to the influence of the vertical accelerations, was the development of a cantilever-type, out-of-plane overturning mechanism at the North central pier in EUC-BUILD-8.2 and EUC-BUILD-8.3, compared to the simple horizontal cracking at mid-height of the same pier in EUC-BUILD-8.1.

The three structures were identical in geometry, and they were constructed using the same batches of materials in a way to reduce the variability in the mechanical characteristics among the specimens. Nevertheless, differences in detailing and environmental conditions during the construction are always expected, resulting in some inevitable variability in the capacity of the structures. Variabilities in structural capacity and the presence of a second horizontal motion component seem to have had a stronger effect on the seismic performance of the three URM building specimens than the vertical accelerations.

The shake-table tests presented in this paper provided a unique dataset that captures at full scale the in-plane and out-of-plane behavior of URM walls, and the influence of flexible diaphragms on the dynamic global response of buildings. Interpretation of the experimental results will constitute the basis for the development and validation of analytical and numerical models to estimate the dynamic response and the parameters for the performance-based seismic assessment of URM buildings and non-structural masonry elements, accounting also for multiple ground-motion components.

7. Acknowledgments

This work is part of the EUCENTRE project *'Study of the vulnerability of masonry buildings in Groningen,'* within the research framework program on hazard and risk of induced seismicity in the Groningen province of the Netherlands, sponsored by the Nederlandse Aardolie Maatschappij BV (NAM). Part of the data post-processing work was financially supported by the ReLUIS-DPC Project 2019-2021 *'Contributions to the*

improvement of standards for existing masonry structures' (Working group 10), funded by the Italian Department of Civil Protection. The authors would like to thank C.G. Lai, A.G. Özcebe, R. Pinho, and H. Crowley for their essential contribution to the selection of the seismic input for the shake-table experiments. The contribution of F. Dacarro, V. Fort, M.P. Scovenna, and the technical staff of the EUCENTRE, who performed the tests, was critical to the project and is gratefully acknowledged. Thanks also go to M. Panatti, S. Sharma, and G. Guerrini for the practical support, and U. Tomassetti for his help in conceiving the design of the specimens.

8. References

[1] Graziotti F, Penna A, Magenes G (2019): A comprehensive in situ and laboratory testing programme supporting seismic risk analysis of URM buildings subjected to induced earthquakes. *Bulletin of Earthquake Engineering*, **17**(8), 4575-4599. DOI: 10.1007/s10518-018-0478-6.

[2] Bommer JJ, Dost B, Edwards B, Stafford PJ, Van Elk J, Doornhof D, Ntinalexis M (2016): Developing an application-specific ground motion model for induced seismicity. *Bulletin. of the Seismological Society of America*, **106**(1), 158-173. DOI: 10.1785/0120150184.

[3] Di Michele F, Cantagallo C, Spacone E (2020): Effects of the vertical seismic component on seismic performance of an unreinforced masonry structure. *Bulletin of Earthquake Engineering*, **18**, 1635-1656. DOI: 10.1007/s10518-019-00765-3.

[4] Liberatore D, Doglioni C, AlShawa O, Atzori S, Sorrentino L (2019): Effects of coseismic ground vertical motion on masonry constructions damage during the 2016 Amatrice-Norcia (Central Italy) earthquakes. *Soil Dynamics and Earthquake Engineering*, 120, 423-435. DOI: 10.1016/j.soildyn.2019.02.015.

[5] Tomassetti U, Correia AA, Candeias PX, Graziotti F, Campos Costa A (2019): Two-way bending out-of-plane collapse of a full-scale URM building tested on a shake-table. *Bulletin of Earthquake Engineering*, **17**(4), 2165-2198. DOI: 10.1007/s10518-018-0507-5.

[6] Graziotti F, Tomassetti U, Sharma S, Grottoli L, Magenes G (2019): Experimental response of URM single leaf and cavity walls in out-of-plane two-way bending generated by seismic excitation. *Construction and Building Materials*, **195**(20), 650-670. DOI: 10.1016/j.conbuildmat.2018.10.076.

[7] Sharma S, Tomassetti U, Grottoli L, Graziotti F (2020): Two-way bending experimental response of URM walls subjected to combined horizontal and vertical seismic excitation. *Engineering Structures*. Accepted for publication.

[8] Kallioras S, Correia AA, Graziotti F, Penna A, Magenes G (2020): Collapse shake-table testing of a clay-URM building with chimneys. *Bulletin of Earthquake Engineering*, **18**(3), 1009-1048. DOI: 10.1007/s10518-019-00730-0.

[9] Vicon Motion Systems (2016): *Vicon Nexus user guide*. Centennial, Colorado, USA. Available at www.vicon.com.

[10] Kallioras S, Grottoli L, Panatti M, Graziotti F (2020): Shake-table experiments on three identical unreinforced clay-brick masonry buildings under uni-, bi-, and tri-directional seismic input motions. *Research Report EUCENTRE*, EUCENTRE, Pavia, Italy. Available at www.eucentre.it/nam-project.

[11] Pinho R (2019). Personal communication. The ground-motion records from the Groningen gas field are available on the KNMI Data Centre platform at data.knmi.nl/datasets.

[12] Den Bezemer T, Van Elk J (2018): Special report on the Zeerijp Earthquake, 8 January 2018. *Research Report NAM*, NAM, Assen, The Netherlands. Available at www.nam.nl/feiten-en-cijfers.

[13] Özcebe AG, Lai L (2019). Personal communication.

[14] Kallioras S, Guerrini G, Tomassetti U, Marchesi B, Penna A, Graziotti F, Magenes G (2018): Experimental seismic performance of a full-scale unreinforced clay-masonry building with flexible timber diaphragms. *Engineering Structures*, **161**, 231-249. DOI: 10.1016/j.engstruct.2018.02.016.

